Chemical Physics 151 (1991) 371–383
North-Holland

A study of the $S_1\,6^1(^1A_2'')$ vibronically excited state of sym-triazine by high-resolution UV laser spectroscopy

Paul Uijt de Haag, W. Leo Meerts
Fysisch Laboratorium, University of Nijmegen, Toernooiveld, 6525 ED Nijmegen, Netherlands

Jon T. Hougen [1]
Molecular Spectroscopy Division, National Institute of Standards and Technology, Gaithersburg, MD 20899, USA

Received 12 October 1990

We have measured the laser induced fluorescence spectrum of the $S_1\,6^1(^1A_2'')\leftarrow S_0(^1A_1')$ vibronic transition in sym-triazine at 317 nm. An instrumental line width of 12 MHz was achieved by the use of a molecular beam in combination with a cw single frequency laser. In this way rotationally resolved spectra were obtained. Furthermore, we have measured the lifetime of some selected ensembles of rovibronic states with a narrow band pulsed laser system. It is shown that the excited $S_1\,6^1(A_2'')$ vibronic state is strongly perturbed by a singlet–triplet interaction. This interaction results in additional lines in the high-resolution spectrum. A nearly complete rotational assignment is given for the transitions to the upper state with rotational quantum number J up to $J=4$ and the rotational constants are derived. No evidence is found for a Jahn–Teller distortion of the rotational states in the $S_1\,6^1(A_2'')$ vibronic state. With some assumptions the singlet-triplet coupling matrix elements were deduced as well as the energy separation between the singlet state and the perturbing triplet state. A singlet–triplet gap of 4800 ± 600 cm^{-1} is estimated.

1. Introduction

The molecule sym-triazine (sym-$C_3H_3N_3$) is the most symmetric azabenzene. In the electronic ground state the molecule belongs to the molecular point group D_{3h}. The vibronic structure of sym-triazine has received a lot of attention over the years and appears to be rather complex [1]. The first excited singlet state is doubly degenerate and of symmetry E″. It arises from a $n(e')\rightarrow\pi^*(e'')$ electron promotion. This electron promotion also gives rise to singlet states of symmetry A_1'' and A_2''. These states are expected in the vicinity of the E″ state. The electronic transition from the ground state $^1A_1'$ to the first excited singlet state $^1E''$ is one-photon electronically forbidden, but two-photon allowed. However, excitation of vibrations of symmetry e′ in the electronic state of symmetry E″ results in vibronic states of symmetry A_2'' ($E''\otimes e'=A_1''$, A_2'' and E″). These states may be subject to a Jahn–Teller distortion [2]. The transition to these vibronically excited states are one-photon allowed whereas coupling of these vibronically excited states to the nearby electronic state with symmetry $^1A_2''$ may enhance the transition probability. An energy level diagram is given in fig. 1.

Several spectroscopic studies on the vibronic structure of the first excited singlet state have been performed with such distinct techniques as one-photon absorption spectroscopy [3], two-photon absorption spectroscopy via photo-acoustic detection [4], one-photon laser induced fluorescence spectroscopy [5–8] and two-photon resonant multi-photon ionization spectroscopy [9]. The analysis of the spectra indicates that the vibrationless electronic transition to the E″ electronic state is situated at 30869 cm^{-1} [4]. The coupling between the $^1E''$ and $^1A_2''$ electronic states is induced by vibrations of mode ν_6. The first strong line in the one-photon laser induced fluorescence spectrum is situated 677 cm^{-1} above the electronic origin and is assigned as the

[1] Nederlandse organisatie voor Wetenschappelijk Onderzoek, visiting scientist University of Nijmegen, Spring 1989.

0301-0104/91/$ 03.50

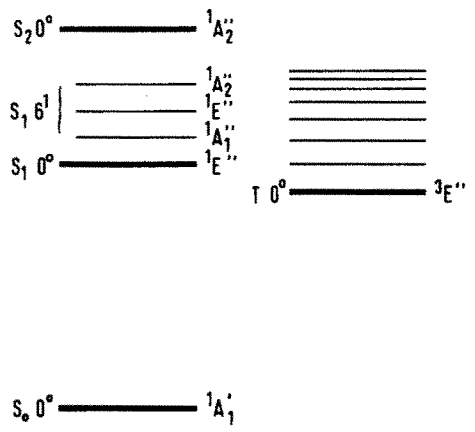

Fig. 1. Energy level diagram of the different vibronic states in sym-triazine. The exact location of the $S_1 6^1$ states with symmetry E'' and A_1'' is not known.

transition to the $S_1 6^1$ state with vibronic symmetry A_2'' [5]. The rotational structure of this line showed nicely resolved P-, Q- and R-branches and indicates a parallel transition, in agreement with the symmetry assignment. However, the spectral resolution was too low to reveal the K substructure. Furthermore no evidence was found for a Jahn–Teller perturbation in this excited state. This resulted in an upper limit for the Coriolis coupling constant between the different vibronic states. It was our aim to examine the Jahn–Teller perturbation in this excited state by measuring a high-resolution spectrum with resolved K substructure.

Besides the coupling to the different nearby singlet states, it is likely that excited vibronic singlet states are also coupled via intersystem crossing to iso-energetic rovibronic states of the lower lying triplet states. However, the available data at the moment are not very conclusive. First of all, neither the origin of the $^3E''$ state is known nor the position of the other low lying triplet states. An absorption band located at 28935 cm^{-1} is attributed to an excited $^3E''\otimes e'$ vibronic state [10]. This indicates that at least one triplet state is located more than 2600 cm^{-1} below the $S_1 6^1(A_2'')$ state. Photoelectron spectra after excitation of the $S_1 6^1(A_2'')$ state were interpreted in terms of a strong intersystem crossing to a triplet state lying at about 5000 cm^{-1} below the $S_1 6^1(A_2'')$ state [9].

Time-resolved fluorescence spectra of the $S_1 6^1(A_2'')$ state showed either a biexponential decay [7] or a single exponential decay [8,11] depending on the experimental conditions. These experimental results were interpreted in the classical terms of a small molecule or an intermediate case molecule with respect to the singlet–triplet coupling [12]. Intriguing was the measured life time dependence on the rotational quantum number of the upper state, J', in one of the experiments [8]. The life time varied from 85 nsec for $J'=1$ to 120 nsec for $J'=6$. However, other experiments showed a more random variation in the measured life time with respect to the excited rotational state [11]. The low quantum yield of sym-triazine indicates that internal conversion to the dense manifold of the singlet ground state and/or intersystem crossing to a dense set of triplet states is the predominant decay channel of the excited state. The dependence of the life time shows that rotation might be important in this process.

We felt that a high-resolution spectrum could reveal the molecular eigenstates, and thus conclusively determine the density of coupled states as well as the rotational effects on the decay process. The high-resolution spectrum of the $S_1 6^1(A_2'')$ state of sym-triazine has been reported previously [11]. However, improvements on the experimental apparatus made it possible to remeasure the spectrum with an improved signal to noise ratio. Furthermore, a home-built pulsed dye amplifier allowed us to measure life times of clearly distinct ensembles of excited rovibronic states. The results of these measurements are also reported here.

2. Experimental

The experimental set-up for the measurement of the high-resolution spectra has been described elsewhere [13]. Only the relevant features are given here. A continuous expansion of sym-triazine (Janssen Chimica, purity 98% and used without further purification) seeded in argon is formed through a nozzle with a diameter of 100 μm. The sym-triazine sample was kept at room temperature (the vapour pressure is 9.6 Torr at 298 K). The backing pressure of the seeding gas was varied between 0.2 and 1 bar. This allowed the recording of the fluorescence spectra at

different rotational temperatures. In this way the rotational assignments of the lines in the spectra were verified. In order to reduce the Doppler line width, the molecular beam is skimmed twice (diameter of the skimmers is 1.5 mm) in a differential pumping system.

At a distance of 30 cm from the nozzle orifice the molecular beam is crossed at right angles by the laser beam. Narrow band UV radiation is generated by intracavity frequency doubling in a single-frequency ring dye laser (a modified Spectra Physics 380D). About 10–15 mW UV radiation with a band width of 3 MHz was obtained by using a Brewster cut $LiIO_3$ crystal. For relative frequency measurements two temperature-stabilized, sealed-off Fabry–Pérot interferometers were used, with free spectral ranges of 150 MHz and 75 MHz, respectively. All frequency scans were performed twice with different scan directions. In this way the frequency measurements were corrected for the residual drift in the interferometers. For the absolute frequency calibration the iodine absorption spectrum was recorded simultaneously [14].

The total undispersed fluorescence was collected by two spherical mirrors and imaged on the photocathode of a photomultiplier (EMI 9789QA). Data processing took place with a standard photon counting system (Ortec Brookdeal 5C1) interfaced with a PDP 11/23+ computer [15]. The instrumental line width in the recorded laser-induced fluorescence spectra amounts to 12 MHz. This line width is mainly determined by the residual Doppler width of the molecular beam in combination with the spatial sensitivity of the collection optics.

For the magnetic field measurements a pair of coils was mounted. The magnetic field was directed parallel to the laser beam. In this way magnetic fields up to 6 mT could be applied.

For the measurement of the time-resolved laser-induced fluorescence spectra a mixture of sym-triazine (room temperature) and argon (or helium) was expanded through a pulsed nozzle. The pulsed valve was a modified Bosch fuel injector with a nozzle diameter of 1 mm. At a distance of 30 mm from the nozzle orifice the molecules were excited by the radiation field of a home-built pulsed dye amplifier (PDA) [16]. The single-frequency output of the continuous-wave ring dye laser was amplified in three dye cells, pumped by the frequency doubled output of a Nd:Yag laser (Quantel 681C-10). The output pulses of the PDA were frequency doubled in an angle-tuned KDP crystal. In this way tunable radiation around 317 nm with a band width of 250 MHz and a pulse energy of 10 mJ was obtained. This means that the spectral brightness of the pulsed dye laser system is about 10^5 times the spectral brightness of the cw ring dye laser system. Therefore, care must be taken to avoid saturation effects. The fluorescence was collected and imaged on the entrance slit of a monochrometer (Oriel 77250) to suppress the stray light of the laser. The transmitted light was detected with a photomultiplier (EMI 9863). Further data processing took place by a LeCroy 9400 digital oscilloscope and a SRS 250 boxcar averager.

3. Results and analysis

3.1. High-resolution experiment

With the high resolution experimental set-up as described, we have measured the laser-induced fluorescence excitation spectrum of the $S_1 6^1(^1A_2'') \leftarrow S_0(^1A_1')$ vibronic transition in sym-triazine at 317 nm. Parts of the spectrum are shown in figs. 2 and 3.

Despite the forbidden nature of the electronic transition and the low quantum yield of the excited vibronic state it was possible to record spectra of good quality. The signal-to-noise ratio in the spectrum amounts to 500 on the strongest lines. The spectrum shows clearly distinct P-, Q- and R-branches, clusters of lines separated by approximately 13 GHz. This is as expected for a parallel transition with the selection rules $\Delta K = K' - K'' = 0$ and $\Delta J = J' - J'' = 0, \pm 1$ [17] (J', K' are the rotational quantum numbers of the excited state and J'', K'' are the rotational quantum numbers of the ground state). In general, each branch up to $J' = 4$ consists of a small number of relatively strong lines. This number corresponds roughly to the number of states with different quantum number K. Besides these strong lines in every branch there are several weak features present. In some branches also some extra relatively strong lines appear (e.g. in the P(4)-branch). Comparison of different transitions to the same upper state clearly reveals that the extra features are due to a perturbation in the excited vibronic state. Starting from the R(4)-branch the spectrum is

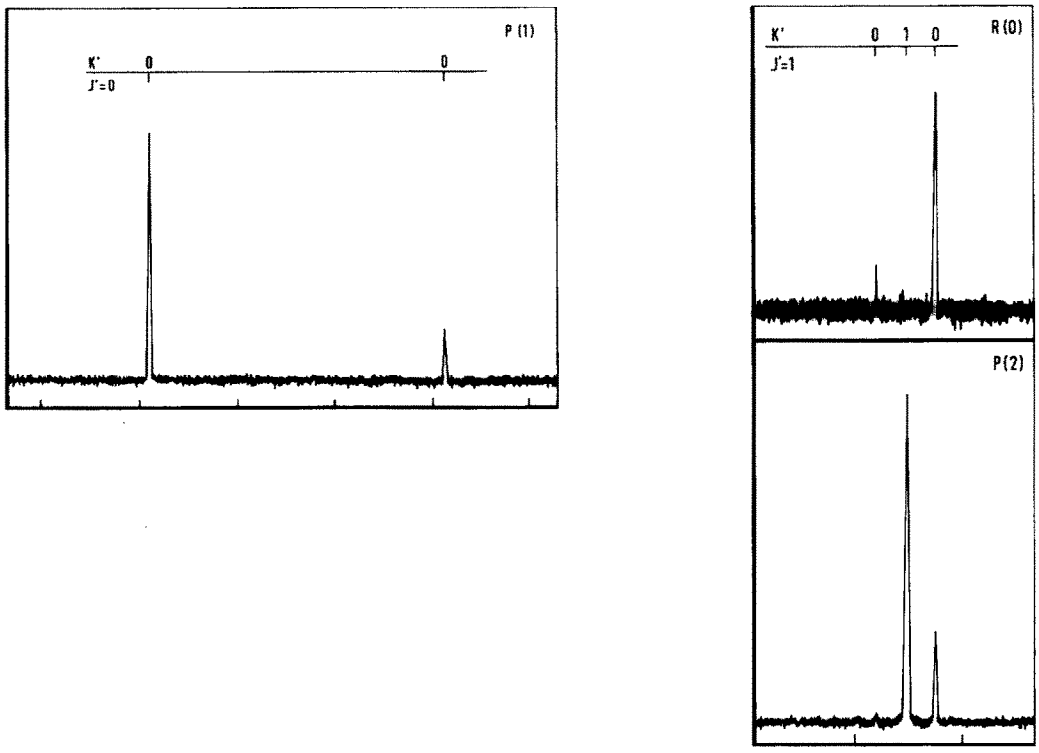

Fig. 2. The P(5)–P(1) and R(0)–R(4) branches of the S_1 $6^1(^1A_2'')\leftarrow S_0(^1A_1')$ vibronic transition in sym-triazine. The rotational identification J', K' of the upper state is given for all assigned lines. All spectra were recorded with 10 mW UV radiation. The backing pressure of the seeding gas argon is 160 Torr for the branches P(5)–P(3) and R(3)–R(4) and 400 Torr for the branches P(2)–P(1) and R(0)–R(2). The frequency is marked every 500 MHz and increases from left to right.

more and more distorted. We have therefore limited our rotational analysis to the branches P(5)–R(3).

The measured line width of the lines in the spectrum is not constant, but varies between the instrumental line width of 12 MHz up to about 50 MHz. A general tendency is that the strong lines have an instrumental line width of 12 MHz and the weak lines have larger line widths.

Rotational analysis

It turned out that it was possible to identify most of the lines in the high-resolution spectrum. The assignments of the rotational quantum numbers were based on the following principles:

Identification of transitions to states with $K'=J'$. An upper state with the rotational quantum numbers J', K' can be accessed via a P-branch transition ($\Delta J=-1$) or via a R-branch transition ($\Delta J=+1$) in case $K'<J'$. However, an upper state with $K'=J'$ can not be accessed via a R-branch transition. In this case the selection rule $\Delta K''=0$ and $\Delta J=+1$ would require a ground state with $K>J''$. Hence the P-branch contains more lines than the R-branch to the upper state with the same J' and the additional lines in the P-branch are unambiguously assigned as transitions to $K'=J'$ states. This method is applied on the combinations R(1)–P(3), R(2)–P(4) and R(3)–P(5).

As the R(0)-branch consists of only one line, it is not possible to apply this method to the R(0)–P(2) combination. However, by means of combination differences between transitions to the same upper state we are able to determine the ground-state rotational constant B''. With the known ground-state rotational constant B'' the frequency difference between the R(0) line and the line with $K''=0$ in the

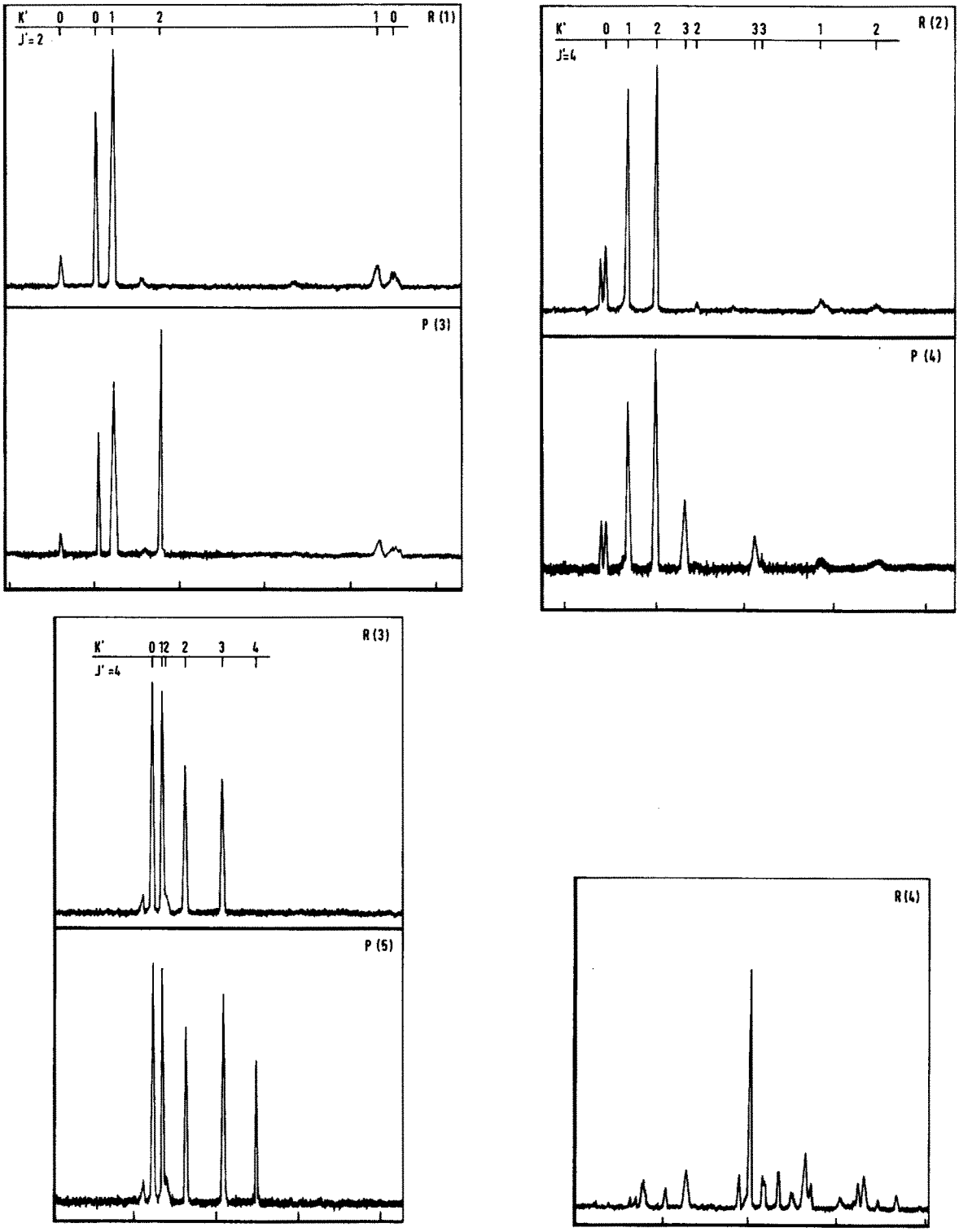

Fig. 2. Continued.

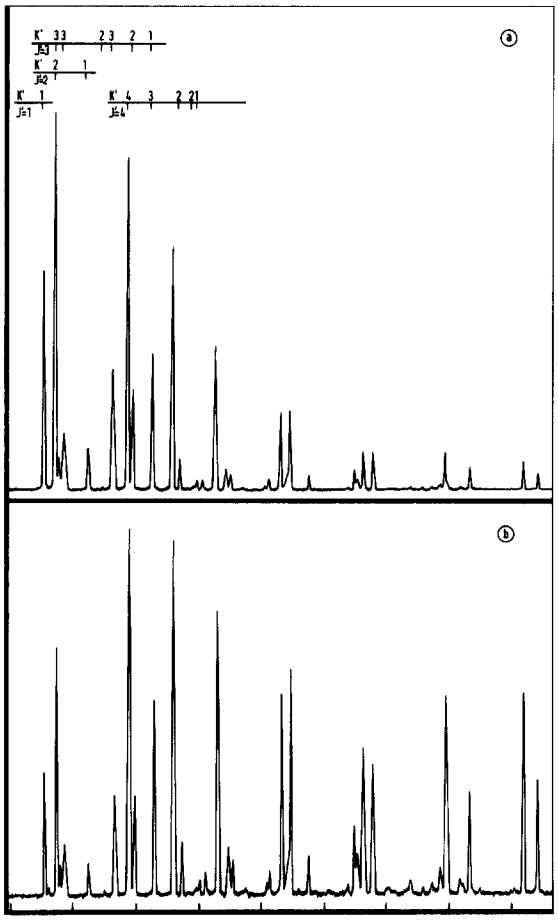

Fig. 3. The Q-branch of the S_1 $6^1(^1A_2'')\leftarrow S_0(^1A_1')$ vibronic transition in sym-triazine recorded at two different backing pressures of the seeding gas Argon, 400 Torr (a) and 150 Torr (b). The frequency is marked every 500 MHz and increases from left to right. The rotational identification of the lines is given for all assigned lines. The difference in rotational temperature is clearly visible.

P(2)-branch can be calculated. In this way the identification of transitions to states with $K'=J'$ is completed.

Identification of transitions to states with $K'\neq J'$. For an asymmetric top molecule it is possible to identify transitions with different quantum number K (where $K=K_{+1}$ (K_{-1}) in the oblate (prolate) symmetric top limit) by a careful comparison of transitions to the same upper state [18]. This method is based on the fact that the asymmetry splitting is dependent on the rotational quantum number J. However, in an oblate symmetric top molecule (like sym-triazine) the rotational energy E_{rot} is given by

$$E_{rot}=BJ(J+1)+(C-B)K^2\,. \qquad (1)$$

In this equation J and K are the rotational quantum numbers and B and C are the rotational constants. In case of a planar symmetric rotor (sym-triazine is planar at least in the vibronic ground state) the relation $B=2C$ holds. It is therefore clear that in a parallel transition the frequency separation between the lines with different K quantum number is the same in the P-branch, Q-branch and R-branch.

The identification of the lines with different quantum number K is for that reason based on the relative intensities of the lines in the spectrum. The relative intensities of single rotational lines in the spectrum, assuming a Boltzmann distribution in the molecular beam, is given by

$$I=I_0\,(2J''+1)\,g_n\,A_{J''K''}\exp(-E_{rot}/kT_{rot})\,\Phi\,. \qquad (2)$$

In this equation J'', K'' are the rotational quantum numbers of the lower state and E_{rot} is the rotational energy of the lower state as given in eq. (1). The rotational temperature of the molecules in the molecular beam is given by T_{rot}. Under the conditions used in this experiment a rotational temperature of 3 K is expected. The nuclear spin statistical weight factor is denoted by g_n and adopts the values [19]

$$\begin{aligned} &K=0 \text{ and } J \text{ odd}: && g_n=56\,,\\ &K=0 \text{ and } J \text{ even}: && g_n=20\,,\\ &K=3p\ (p \text{ integer}\neq 0): && g_n=76\,,\\ &K=3p\pm 1\ (p \text{ integer}\neq 0): && g_n=70\,. \end{aligned} \qquad (3)$$

$A_{J''K''}$ are the Hönl–London factors. In case of a parallel band these are given by [17]

$$\begin{aligned} A_{J''K''}&=\frac{J''^2-K''^2}{J''(2J''+1)}, && \Delta J=-1\,,\\ A_{J''K''}&=\frac{K''^2}{J''(J''+1)}, && \Delta J=0\,,\\ A_{J''K''}&=\frac{(J''+1)^2-K''^2}{(J''+1)(2J''+1)}, && \Delta J=+1\,. \end{aligned} \qquad (4)$$

I_0 is the normalized intensity and k is the Boltzmann

constant. Finally the factor Φ takes the perturbations in the upper state into account and denotes the relative excitation and fluorescence efficiency of a certain upper rovibronic state. The presence of this factor makes it impossible to fit the relative intensities in the spectrum to a normal Boltzmann distribution.

Eq. (2) is correct as long as all nuclear spin functions are allowed to relax to the same rotational ground state. It is well known that nuclear spin is conserved in the cooling process. This means that eq. (2) holds only within one nuclear spin symmetry group. However, calculations only show a noticeable deviation from eq. (2) at temperatures below 1 K. With the typical rotational temperature of 3 K in our molecular beam eq. (2) is assumed to be valid.

For the identification of the rotational quantum numbers in the spectrum of sym-triazine use has been made of eq. (2) in two ways. Although the relative intensities contain an unknown factor Φ it is still possible to compare the intensities of transitions to the same upper state. Especially corresponding lines in the Q- and P-branch have completely different Hönl–London factors. Most identifications are based on this principle. Furthermore, all spectra were measured with two different backing pressures (0.2 bar and 0.5 bar) of the seeding gas argon, corresponding to two different rotational temperatures in the molecular beam. This is clearly visible in fig. 3. In this way the relative intensities of the transitions with different quantum number K are varied within one branch. This method is however less suited for low K values due to the small difference in rotational energy.

With these two methods a nearly complete assignment of the rovibronic transitions in the $S_1\,6^1(^1A_2'')\leftarrow S_0(^1A_1')$ band system of sym-triazine was achieved for the P(5)–R(3) branches. The identifications are given in figs. 2 and 3. With this identification the rotational constants of sym-triazine in the ground and excited vibronic state could be deduced.

The ground-state rotational constant B'' is found by means of combination differences between the P- and R-branches and is given in table 1. The error in this rotational constant is determined by the uncertainty in the free spectral range of the used Fabry–Pérot interferometers and residual drift effects. The value of the ground-state rotational constant derived from our high-resolution spectrum is in reasonable agreement with the value $B''=6434$ MHz derived from rotational Raman spectroscopy [20].

The rotational constant B' of the vibronic excited state $S_1\,6^1(A_2'')$ is more difficult to obtain due to the perturbations in the vibronic excited state. It is immediately clear from the reversed K structure in the P(2)-branch with respect to the other branches (see fig. 2) that it is not possible to fit the normal symmetric top energy formulas. However, if we assume that the strong lines are more or less randomly shifted from their symmetric top positions by the perturbation, we can try to fit these lines to the normal symmetric top energy formulas. The results are given in tables 1 and 2. The observed line frequencies listed in table 1 correspond to the strongest lines of the transitions. Exceptions are the line position for the P(1)-branch and the $K'=3$ line position for the P(3)-branch. In these cases the intensity weighted center of gravity of the lines is used.

The observed frequencies were fitted to the energy expressions of eq. (1) for both the ground and upper vibronic state. The relation $B=2C$ was used in both states and the ground-state rotational constant B'' was kept fixed. Therefore, only the center frequency of the transition ν_0 and the rotational B' constant of the upper state were fitted. The result of the fit is given in table 2. The error in the excited state constant is determined by the accuracy of the fit. The error in the center frequency ν_0 of the transition is determined by the combination of the accuracy of the fit and the accuracy in the determination of the peak positions of the iodine absorption lines. It is clear from table 1 that the deviations between the observed frequencies and the calculated frequencies are of the order of 100 MHz. This is well above the experimental accuracy. However, if we would take the intensity weighted center of gravity of the lines with the same rotational quantum numbers, the line positions would shift over 200 MHz. Hence we cannot expect a more accurate fit.

It is well known that a degenerate vibration in a degenerate electronic state (like the excited vibronic state in sym-triazine) is subjected to a Jahn–Teller distortion. In this case the rotational energy is no longer given by eq. (1), but [2,21]

$$E_{\mathrm{rot}}=BJ(J+1)+(C-B)K^2 \pm\sqrt{\tfrac{1}{4}(\Delta\nu)^2+4C^2K^2\zeta_{\mathrm{eff}}^2}\,. \qquad (5)$$

Table 1
Observed and calculated rovibronic frequencies of the $S_1\,6^1(^1A_2'')\leftarrow S_0(^1A_1')$ vibronic transition in sym-triazine relative to the center frequency $\nu_0 = 31546.70\ cm^{-1}$.

Observed frequency (MHz)	Calculated frequency (MHz)	obs. − calc. (MHz)	J''	K''	J'	K'
−65742	−65758	16	5	0	4	0
−65687	−65724	37	5	1	4	1
−65554	−65624	70	5	2	4	2
−65329	−65456	127	5	3	4	3
−65136	−65221	85	5	4	4	4
−52587	−52338	−249	4	0	3	0
−52470	−52304	−166	4	1	3	1
−52313	−52204	−109	4	2	3	2
−52087 [a)]	−52036	−51	4	3	3	3
−39179	−39052	−127	3	0	2	0
−39086	−39019	−67	3	1	2	1
−38823	−38919	96	3	2	2	2
−25722	−25900	178	2	0	1	0
−25856	−25867	11	2	1	1	1
−12817 [a)]	−12883	66	1	0	0	0
−1288	−1307	19	4	1	4	1
−1152	−1202	55	4	2	4	2
−930	−1039	109	4	3	4	3
−779	−903	124	3	2	3	2
−740	−805	65	4	4	4	4
−553	−503	−50	3	3	3	3
−427	−369	−58	2	1	2	1
−166	−268	102	2	2	2	2
−77	−101	24	1	1	1	1
12938	12749	189	0	0	1	0
25250	25365	−115	1	0	2	0
25343	25398	−55	1	1	2	1
37599	37945	−246	2	0	3	0
37717	37879	−162	2	1	3	1
37874	37979	−105	2	2	3	2
50193	50193	0	3	0	4	0
50247	50226	21	3	1	4	1
50381	50327	54	3	2	4	2
50606	50495	111	3	3	4	3

[a)] These lines are combinations of different lines in the spectrum. See text.

In this equation $\Delta\nu$ is the energy splitting between the A_1'' and A_2'' vibronic states and ζ_{eff} is the effective vibronic angular momentum. This energy expression reduces for very large $\Delta\nu$ to the normal symmetric top energy expression (eq. 1). For very small energy splittings $\Delta\nu$ eq. (5) reduces to

$$E_{rot} = BJ(J+1) + (C-B)K^2 \pm 2CK\zeta_{eff}. \qquad (6)$$

In case of intermediate energy splittings expansion of eq. (5) leads again to eq. (1), but with slightly different rotational constants.

In order to determine any effects of a Jahn–Teller distortion in the excited vibronic state $S_1\,6^1(A_2'')$ in sym-triazine, we have fitted the frequencies listed in

Table 2
Molecular constants of the sym-triazine molecule in the electronic ground state S_0 and the vibronically excited state $S_1\,6^1(A_2'')$.

B''	6442 ±4	MHz
B'	6375 ±10	MHz
ν_0	31456.70±0.01	cm^{-1}

table 1 both to eq. (1) and to eq. (6) as the energy expressions for the excited state. However, no significant improvement of the fit is achieved. We conclude therefore that there is no evidence for a Jahn–Teller effect in the high-resolution spectrum of the $S_1 6^1(A_2'')$ vibronic state.

Magnetic field measurement

As already stated, the high-resolution spectrum of the $S_1 6^1(^1A_2'') \leftarrow S_0(^1A_1')$ vibronic transition in sym-triazine appears to be perturbed. This is evidently shown by the extra lines in the spectrum and the deviations of the observed frequencies with respect to the calculated symmetric rotor line positions. The similarity of the view of the P- and the R-branch to the same upper state clearly reveals that the perturbations occur in the $S_1 6^1(A_2'')$ excited vibronic state. However, the nature of the perturbing state is not known since many singlet and triplet vibronic states are expected in the vicinity of the excited state. We have therefore measured a part of the high-resolution spectrum in a magnetic field. In fig. 4 a part of the R(2)-branch is shown with magnetic field strengths up to 6 mT. It is clearly seen that the view of the spectrum is completely altered at even moderate magnetic fields. This establishes that the perturbing state is a triplet state, similar to the situation in other azabenzenes like pyrimidine and pyrazine. The magnetic field spectra are too complex for a profound analysis.

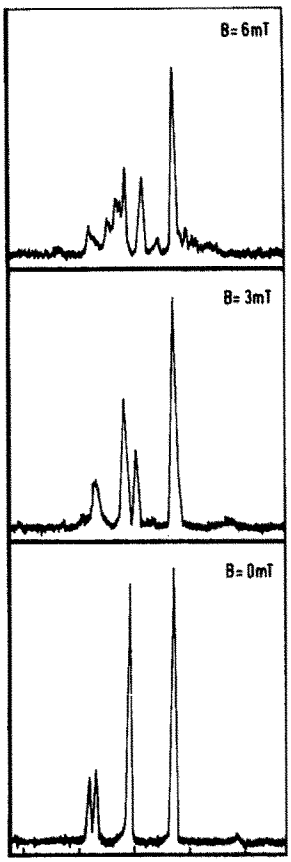

Fig. 4. Part of the R(2)-branch of the $S_1 6^1(^1A_2'') \leftarrow S_0(^1A_1')$ vibronic transition in sym-triazine recorded with different magnetic fields.

3.2. Life time measurements

It was shown in the high-resolution experiments that the line widths varied between 12 MHz (the instrumental line width) up to 50 MHz. The strong lines tend to have the instrumental limited line width, where the weak lines tend to have a broader line width. However, due to the low signal to noise ratio it was not possible to determine conclusively whether the lines were broadened homogeneously or inhomogeneously. Comparison of several scans indicates that the lines are presumably inhomogeneously broadened, i.e. consist of a number of lines overlapping within the instrumental line width.

If the weak lines are broadened homogeneously, a measured line width of 50 MHz would correspond to a life time of 3 nsec for the excited state. As the known life time is about 100 nsec for an excited ensemble of rovibronic states [7,8,11] this would indicate that the weak lines exhibit a strong non-radiative decay. Hence the quantum yield of the broadened lines is at least a factor 30 less than the quantum yield of the strong lines. This would change the interpretation of the spectrum tremendously. Furthermore, the strong lines are transitions to molecular eigenstates with mainly singlet character where the weak lines are expected to be transitions to molecular eigenstates with mainly triplet character (see Appendix). Hence a homogeneous broadening of the weak lines would indicate a strong non-radiative decay of the triplet states. There are models for the intersystem crossing in pyrazine proposed based on such a strong triplet decay rate [22].

To determine conclusively whether the lines are broadened homogeneously or inhomogeneously, we have measured the life times of some selected ensembles of rovibronic states with the pulsed experimental set-up as described. The life time measurements were made in the R(1)-branch (see fig. 2). The R(1)-branch consists of two clusters of lines separated by about 1600 MHz, i.e. five times the instrumental resolution in the pulsed experiment. On the low-frequency side three lines are found with a line width between 12–15 MHz. On the high-frequency side two relatively weak lines are found with line widths of 40 and 50 MHz.

Fig. 5 shows the spectrum of the R(1)-branch measured with the pulsed experimental set-up. The spectrum is obtained with a backing pressure of 0.9 bar of the seeding gas argon. In order to avoid saturation effects the output of the pulsed dye amplifier was attenuated and a pulse energy of only 30 μJ was used. The spectrum clearly shows two lines, about 1560 MHz apart and with line widths of 350 MHz. The experimental width of the lines is determined by the combination of the Doppler line width in the molecular beam and the laser band width of the pulsed dye amplifier system. The separation of 1560 MHz of the two lines is in good agreement with the separation of the two groups of lines in the high-resolution spectrum. Furthermore, the intensity ratios of the lines measured with the pulsed laser system is within the experimental accuracy in accord with the intensity ratio of the two groups of lines in the high-resolution spectrum, taking the line widths into account. As the spectrum of fig. 5 is measured in a time interval between 40 and 180 nsec after the laser pulse, this clearly proves that the life times of the two lines are comparable. Hence the lines in the high-resolution spectrum are broadened inhomogeneously.

We have measured the decay curves after excitation of line ① and after excitation of line ②. The results are given in fig. 6. The life times τ measured

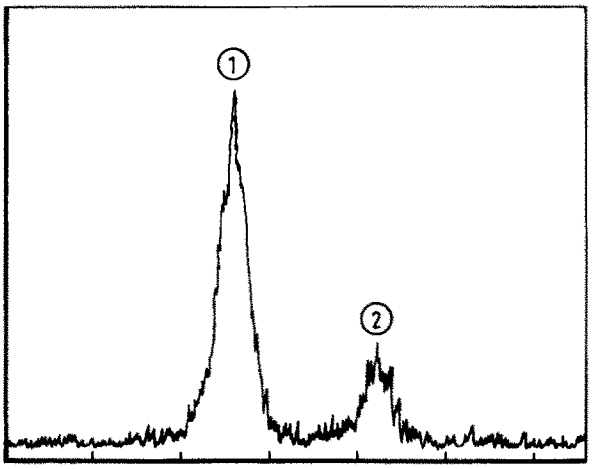

Fig. 5. The R(1)-branch of the $S_1 6^1(^1A_2'') \leftarrow S_0(^1A_1')$ vibronic transition in sym-triazine recorded with the narrow-band pulsed laser system. The backing pressure of the seeding gas argon was 0.9 bar, and the pulse energy of the laser was 30 μJ. The frequency is marked every 500 MHz and increases from left to right. The fluorescence is collected with a gate between 40 and 180 nsec after the stray light pulse of the laser.

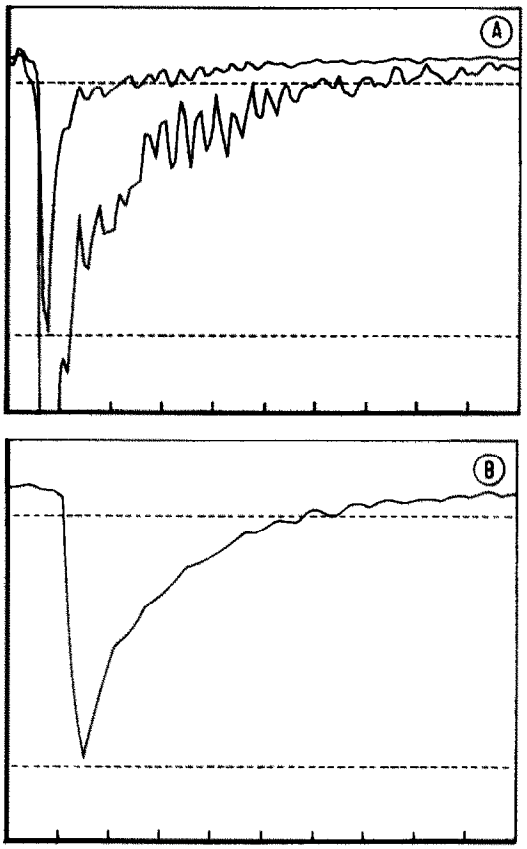

Fig. 6. Fluorescence decay curves after excitation of the lines in the R(1)-branch. The measured life times are $\tau = 140 \pm 20$ nsec [(A) excitation of the weak line] and $\tau = 100 \pm 10$ nsec [(B) excitation of the strong line]. Markers are indicated every 100 nsec in figure (A) and every 50 nsec in figure (B).

from these decay curves are $\tau = 100 \pm 10$ nsec after excitation of line (1) and $\tau = 140 \pm 20$ nsec after excitation of line (2). These life times are in good agreement with the life times measured previously [7,8,11].

These measured life times clearly reveal that the broadening of weak lines in our high-resolution spectrum is due to several overlapping transitions. It is also shown that the life times of the two lines are comparable and do not scale with the intensity. This indicates (see the Appendix) that the triplet states coupled to the singlet state have a (non-radiative) decay rate comparable to the singlet state decay rate. This result is also found in pyrazine [23] and pyrimidine [24].

4. Discussion

It has been shown that the high-resolution spectrum of sym-triazine is strongly perturbed. We have identified the perturbing state as a triplet state. The basic principles of a singlet state interacting with a set of triplet states are well known and they are summarized in the Appendix.

We can use the rotational assignment of the high-resolution spectrum to calculate the coupling matrix elements V_{st} between the singlet state and the triplet states for every set of lines with the same quantum numbers J', K'. In this the unassigned lines in the spectrum are omitted. The coupling matrix elements are given in table 3. It is assumed in the calculation of these matrix elements that the laser-induced fluorescence intensities directly reflect the absorption intensities. Furthermore, in the deconvolution procedure the different line widths in the spectrum were not taken into account and the peak heights were used as a measure of the intensities. We can compare the singlet–triplet coupling matrix elements deduced for sym-triazine (table 3) with the singlet–triplet coupling matrix elements of pyrazine [18,23] and pyrimidine [24]. We conclude that the average singlet–triplet coupling strength V_{st} in sym-triazine is comparable to the average coupling strength in pyrazine and much larger than the average coupling strength in pyrimidine. However it must be noticed that the much weaker signal to noise ratio in the spectrum of sym-triazine relative to the spectrum of pyrimidine has the tendency to suppress the small coupling matrix elements.

Table 3
Singlet–triplet coupling matrix elements V_{st} in the vibronic excited state $S_1 6^1(A_2'')$ of sym-triazine

J'	K'	V_{st} (MHz)
0	0	590
1	0	64
2	0	75, 430
2	1	415
3	1	232
3	2	38, 174
3	3	25, 198
4	2	35

As the coupling strengths in sym-triazine and pyrazine are comparable, we can use the density of lines in the spectrum to estimate the singlet–triplet gap. The density of lines in the spectrum of sym-triazine is about one-third of the density of lines in the spectrum of pyrazine. In this we take the lower signal-to-noise ratio into account. We can calculate with the formula of Haarhoff [25] the magnitude of the singlet–triplet gap in sym-triazine at which the calculated density of triplet states is one-third of the calculated density of triplet states in pyrazine. Using the ground-state vibrational frequencies for both molecules the energy separation between the excited $S_1 6^1(A_2'')$ state in sym-triazine and the interacting triplet state is calculated to be 4800 cm^{-1}. If we assume a factor three as the uncertainty in the estimated density of lines (i.e., the density of lines in the spectrum of sym-triazine is between one and one-tenth of the density of lines in the spectrum of pyrazine) the error in the calculated singlet–triplet gap is 600 cm^{-1}. Hence we conclude that the energy separation between the $S_1 6^1(A_2'')$ state and the triplet state is 4800 ± 600 cm^{-1}. This result is in excellent agreement with the singlet–triplet gap deduced from the electron spectroscopy [9].

We have shown that most weak lines in the high-resolution spectrum are in fact clusters of several overlapping transitions. A same clustering of lines has been observed in pyrazine [18]. The question arises why the triplet states appear in clusters. A possible mechanism assumes that the hyperfine splittings in the triplet state of sym-triazine are in the order of 10

MHz, i.e. observable in our high-resolution spectrum. This mechanism is proposed to explain the experimental determined density of states in pyrazine [18]. This would suggest that different hyperfine components of the triplet state interact with different hyperfine components of the singlet state. In this way a broadening of a few MHz of the almost pure singlet molecular eigenstate is expected. Such a broadening is in fact observed in our high-resolution spectrum of sym-triazine (e.g. the transition to the $(J', K') = (2, 1)$ excited state). However, it was not possible to measure such an effect for every state as the additional broadening is small compared to the instrumental line width. The nature of the clustering of lines in sym-triazine remains therefore still uncertain.

Acknowledgements

We would like to thank M. Drabbels, M. Ebben and J. Heinze for experimental assistance. This work was financially supported by the Dutch Organisation for Scientific Research (FOM/NWO).

Appendix: a simple theory of molecular eigenstates

The case of a singlet state coupled to a set of triplet states can be described in a simple model with the effective Hamiltonian H

$$H = H_0 + \sum_t V_{st}\,, \tag{A.1}$$

here the zero order Hamiltonian H_0 is diagonal on the basis formed by the zero order singlet state $|s\rangle$ and the zero order triplet states $\{|t\rangle\}$. The singlet state $|s\rangle$ is coupled to the set of triplet states $\{|t\rangle\}$ by the matrix elements V_{st}.

The effective Hamiltonian H is diagonal on the basis of the molecular eigenstates $|n\rangle$. These molecular eigenstates can be expanded in the zero-order states

$$|n\rangle = c_{ns}|s\rangle + c_{nt}|t\rangle \tag{A.2}$$

In this way the decay rate γ_n of the molecular eigenstate $|n\rangle$ is given in terms of the zero-order singlet decay rate γ_s and the zero-order triplet decay rates γ_t by

$$\gamma_n = |c_{ns}|^2\gamma_s + \sum_t |c_{nt}|^2\gamma_t\,. \tag{A.3}$$

The decay rate γ can have both radiative and non-radiative contributions, denoted by γ^r and γ^{nr} respectively.

The zero-order singlet state $|s\rangle$ is assumed to carry the oscillator strength from the ground state. Hence the absorption intensity A_n of the molecular eigenstate $|n\rangle$ is proportional to the amount of singlet character in the molecular eigenstate

$$A_n \propto |c_{ns}|^2\,. \tag{A.4}$$

In a laser-induced fluorescence experiment however the intensity I_n of a molecular eigenstate $|n\rangle$ is proportional to the absorption intensity times the quantum yield of the excited state

$$I_n \propto |c_{ns}|^2 \frac{\gamma_n^r}{\gamma_n}\,. \tag{A.5}$$

It is easy to see that in case the singlet decay rate is much larger than the triplet decay rate ($\gamma_s \gg \gamma_t$) the laser-induced fluorescence intensity I_n is proportional to the absorption intensity A_n and also proportional to the decay rate γ_n of the excited state.

In the case that one singlet state is coupled to a set of triplet states it is possible to deduce the positions of the zero-order states $|s\rangle$, $\{|t\rangle\}$ and the coupling matrix elements V_{st} via a deconvolution procedure [26]. In this procedure the line positions and the absorption intensities of the molecular eigenstates are required. The situation where one singlet state is present in the spectrum is encountered only in the P(1)- and R(0)-branch in case of a parallel transition. Hence the deconvolution procedure can be applied directly to the lines in the P(1)- and R(0)-branch. In the other branches a rotational assignment is needed and the deconvolution procedure is made for every set of J', K' lines independently. However, in the case that the zero-order triplet states are split by hyperfine interactions or magnetic field effects the deconvolution procedure is not valid when applied to the whole set of J', K' lines. This is caused by the fact that the different components of the triplet states interact with the corresponding (overlapping) components of the singlet state. Therefore, effectively more than one singlet state is present. Application of the deconvolution procedure to the whole set of lines in the spectrum leads in this case to an underestimation of the coupling matrix elements V_{st}.

References

[1] For a review see, K.K. Innes, I.G. Ross and W.R. Moomaw, J. Mol. Spectry. 132 (1988) 492.

[2] G. Herzberg, Molecular Spectra and Molecular Structure, Vol. 3 (Van Nostrand, New York, 1966).

[3] Y. Udagawa, M. Ito and S. Nagakura, J. Mol. Spectry. 39 (1971) 400.

[4] J.D. Webb, K.M. Swift and E.R. Bernstein, J. Chem. Phys. 73 (1980) 4891.

[5] M. Heaven, T. Sears, V.E. Bondybey and T.A. Miller, J. Chem. Phys. 75 (1981) 5271.

[6] A.E.W. Knight and C.S. Parmenter, Chem. Phys. 43 (1979) 257.

[7] N. Ohta and H. Baba, Chem. Phys. Letters 84 (1981) 308; ibid., Chem. Phys. 82 (1983) 41; ibid., Chem. Phys. Letters 106 (1984) 382.

[8] H. Saigusa and E.C. Lim, J. Chem. Phys. 78 (1983) 91.

[9] J.B. Pallix and S.D. Colson, Chem. Phys. Letters 119 (1985) 38.

[10] D.A. Wiersma, Chem. Phys. Letters 16 (1972) 517.

[11] B.J. van der Meer, Thesis (1985).

[12] G.W. Robinson, J. Chem. Phys. 47 (1967) 1967.

[13] W.A. Majewski and W.L. Meerts, J. Mol. Spectry. 104 (1984) 271.

[14] S. Gerstenkorn and P. Luc, Atlas du Spectroscopie d'Absorption de la Molecule d'Iode (Centre National de la Recherche Scientifique, Orsay, 1978);
S. Gerstenkorn and P. Luc, Rev. Phys. Appl. 14 (1979) 791.

[15] W.M. van Herpen, W.L. Meerts and A. Dymanus, J. Chem. Phys. 87 (1987) 182.

[16] E. Cromwell, T. Trickl, Y.T. Lee and A.H. Kung, Rev. Sci. Instr. 60 (1989) 2888.

[17] G. Herzberg, Molecular Spectra and Molecular Structure, Vol. 2 (Van Nostrand, New York, 1966).

[18] W. Siebrand, W.L. Meerts and D.W. Pratt, J. Chem. Phys. 90 (1989) 1313.

[19] A. Weber, J. Chem. Phys. 73 (1980) 3952.

[20] J.E. Lancaster and B.P. Stoicheff, Can. J. Phys. 34 (1956) 1016.

[21] J.T. Hougen, J. Chem. Phys. 38 (1963) 1167.

[22] A. Amirav, Chem. Phys. 108 (1986) 403.

[23] W.M. van Herpen, W.L. Meerts, K.E. Drabe and J. Kommandeur, J. Chem. Phys. 86 (1987) 4396.

[24] J.A. Konings, W.A. Majewski, Y. Matsumoto, D.W. Pratt and W.L. Meerts, J. Chem. Phys. 89 (1988) 1813.

[25] P.C. Haarhoff, Mol. Phys. 7 (1963) 101.

[26] W.D. Lawrance and A.E.W. Knight, J. Phys. Chem. 89 (1985) 917.